



Interflow dynamics on a low relief forested hillslope: Lots of fill, little spill [☆]



Enhao Du ^{a,e,*}, C. Rhett Jackson ^a, Julian Klaus ^{b,f}, Jeffrey J. McDonnell ^{b,c}, Natalie A. Griffiths ^d, Margaret F. Williamson ^{a,1}, James L. Greco ^{a,2}, Menberu Bitew ^a

^a Warnell School of Forestry and Natural Resources, University of Georgia, Athens, GA 30602, United States

^b Global Institute of Water Security, University of Saskatchewan, Canada

^c School of Geosciences, University of Aberdeen, UK

^d Climate Change Science Institute and Environmental Sciences Division, Oak Ridge National Laboratory, Oak Ridge, TN 37831, United States

^e Climate Science Department, Lawrence Berkeley National Laboratory, Berkeley, CA 94720, United States

^f Catchment and Eco-hydrology Research Group, Luxembourg Institute of Science and Technology, Esch-sur-Alzette, Luxembourg

ARTICLE INFO

Article history:

Received 16 September 2014

Received in revised form 30 June 2015

Accepted 19 January 2016

Available online 27 January 2016

This manuscript was handled by Laurent Charlet, Editor-in-Chief, with the assistance of Tamotsu Kozaki, Associate Editor

Keywords:

Interflow
Argillic layer
Low relief
Fill-and-spill

SUMMARY

We evaluated the occurrence of perching and interflow over and within a sandy clay loam argillic horizon within first-order, low-relief, forested catchments at the Savannah River Site (SRS) in the Upper Coastal Plain of South Carolina. We measured soil hydraulic properties, depths to the argillic layer, soil moisture, shallow groundwater behavior, interflow interception trench flows, and streamflow over a 4-year period to explore the nature and variability of soil hydraulic characteristics, the argillic “topography”, and their influence on interflow generation. Perching occurred frequently within and above the restricting argillic horizons during our monitoring period, but interflow was infrequent due to microtopographic relief and associated depression storage on the argillic layer surface. High percolation rates through the argillic horizon, particularly through soil anomalies, also reduced the importance of interflow. Interflow generation was highly variable across eleven segments of a 121 m interception trench. Hillslopes were largely disconnected from stream behavior during storms. Hillslope processes were consistent with the fill-and-spill hypothesis and featured a sequence of distinct thresholds: vertical wetting front propagation to the argillic layer; saturation of the argillic followed by local perching; filling of argillic layer depressions; and finally connectivity of depressions leading to interflow generation. Analysis of trench flow data indicated a cumulative rainfall threshold of 60 mm to generate interflow, a value at the high end of the range of thresholds reported elsewhere.

Published by Elsevier B.V.

1. Introduction

Subsurface stormflow or interflow (defined here as shallow slope-parallel flow over an impeding horizon) has been studied on forested hillslopes since Engler (1919) (Bachmair and Weiler,

2011; Weiler et al., 2005). Hewlett (1961) demonstrated the potential importance of interflow to watershed processes by examining interflow and drainage dynamics on re-packed hillslope troughs. Subsequently, early conceptualizations of hillslope flow processes assumed that the topography of the impeding layer was similar to that of the soil surface as in the classic schematic by Atkinson (1978) or the seminal simulations by Zaslavsky and Sinai (1981). Hewlett and Hibbert (1967) later used a multi-catchment comparison to show the overarching importance of soil depth on interflow magnitude and catchment runoff production. Since then, studies have examined the role of topographic convergence on interflow patterns (Anderson and Burt, 1978), the role of soil pipes (Mosley, 1979), and interflow mixing and displacement (Pearce et al., 1986). A continuing issue for physically-based hydrologic modeling is the need to understand how the mismatch between

[☆] Note: This manuscript has been authored by UT-Battelle, LLC, under Contract No. DE-AC05-00OR22725 with the U.S. Department of Energy. The United States Government retains and the publisher, by accepting the article for publication, acknowledges that the United States Government retains a non-exclusive, paid-up, irrevocable, world-wide license to publish or reproduce the published form of this manuscript, or allow others to do so, for the United States Government purposes.

* Corresponding author at: Climate Science Department, Lawrence Berkeley National Laboratory, Berkeley, CA 94720, United States. Tel.: +1 805 204 7437.

E-mail address: enhaodu@gmail.com (E. Du).

¹ Current address: Peace Corps, Washington, D.C. 20526, United States.

² Current address: ADA Engineering, Tampa, FL 33606, United States.

our knowledge of surface and subsurface topography affects our predictions of hillslope behavior.

In the past two decades, the use of geophysical techniques to study hillslopes has revealed that subsurface topography can differ substantially from surface topography (McDonnell et al., 1996). This realization led to new concepts of interflow generation via filling and spilling of depressions created by subsurface topography (Spence and Woo, 2003). Tromp van Meerveld and McDonnell (2006c) demonstrated for the instrumented hillslope at the Panola Mountain Research Watershed, Georgia, USA that downslope flow proceeded along subsurface interfacial dendritic drainage networks that had to fill, spill, and connect as later modeled by Hopp and McDonnell (2009). Since then, others have observed fill and spill processes in other environments and found that bedrock topography more strongly controls hydraulic gradient than surface topography in flat terrain (Devito et al., 2005). Similarly, Ali et al. (2011) found that subsurface storage is a more sensitive surrogate for discharge in a steep headwater catchment than surface storage. Spatial analysis of runoff source area in moderately sloping catchments revealed that runoff production is controlled by connectivity of shallow groundwater among the hillslope, riparian zone, and stream (Jencso et al., 2009). These findings indicate subsurface topography of the impeding layers may play a more important role than surface topography on storm water partitioning and redistribution in moderately sloping catchments.

While the factors causing interflow are well studied in steep catchments, the dynamics of interflow in low-angle forested catchments are less understood. Experimental work has shown that interflow in low to moderate angle topography can occur over Bt and Bw horizons (layers of clay or iron accumulation, respectively) (Beasley, 1976; Newman et al., 1998; Wilson et al., 1990) and fragipans (McDaniel et al., 2008; Parlange et al., 1989). Modeling studies have shown that the effect of subsurface concavities is diminished as slope increases (Hopp and McDonnell, 2009) as water spills more readily over the downslope lip of each concavity. In low angle forested slopes with deep (e.g., >100 m) underlying bedrock, the subsurface topography has not been defined by differential weathering or shallow landsliding but rather by biological processes such as windthrow (Gabet and Mudd, 2010; Ulanova, 2000) and animal burrowing (Nearby et al., 2009) and also irregularities in soil weathering and illuviation of fine particles. Thus, the spill pathways connecting local concavities are likely to be random and dissimilar to fluvial pathways. If, however, subsurface pathways are dominated by macropore networks created by root systems, then subsurface topography likely becomes a control on flow networks (Tromp van Meerveld and McDonnell, 2006b). Because of these complexities, interflow influenced by the presence of an argillic clay horizon (Bt horizons) ranges from frequent and substantial (Beasley, 1976; Wilson et al., 1990) to rare and inconsequential (Buttle and McDonald, 2002; Redding and Devito, 2010). Evaluating the contrasts in flow behavior among hillslopes with different steepness and lithology allows us to understand and predict the relative balance of fill and spill (McDonnell, 2013).

Here we present new work that examines the controls on perching (here defined as a subsurface water table that builds up temporarily over restricting layers) and interflow generation over and within a sandy argillic horizon on low angle slopes (less than 5%) within forested catchments in the Sandhills of the Upper Coastal Plain, South Carolina, USA. We quantified the variability of the argillic topography and saturated hydraulic conductivities of both the Bt horizon and the overlying A and E horizons, the spatial variability of interflow across a 120 m long interflow interception trench divided into 11 segments, as well as perching within and on the argillic layer using piezometers on the hillslope above the trench. The following questions guided our research: (1) Do

low angle slopes exhibit similar threshold and fill-and-spill behavior as steeper hillslopes? (2) How variable are the subsurface topography and hydraulic characteristics of the impeding argillic layer? (3) Does surface topography predict the frequency of perching and interflow production across the slope?

2. Study site

The study was conducted in three adjacent first order catchments, with the majority of research conducted on a single catchment and most data collected from 2008 to 2011. All three catchments are tributaries to Fourmile Branch on the U.S. Department of Energy (DOE) Savannah River Site (SRS) within the Aiken plateau of the Upper Atlantic Coastal Plain (Fig. 1) in South Carolina, USA. The SRS site was in row-crop, agriculture, featuring terracing and shallow gullies prior to acquisition and reforestation by the Atomic Energy Commission (a predecessor to DOE) in 1950 (Kilgo and Blake, 2005). Annual precipitation at the site is approximately 1220 mm distributed evenly throughout the year, while potential evapotranspiration is approximately 1400 mm. The weather is characterized by long, hot summers with an average daily maximum temperature of 32.3 °C and high intensity thunderstorms and relatively mild winters with an average temperature of 8.6 °C (Rebel, 2005) and frontal rainfall.

The headwater catchments are characterized by gently rolling hills with average slopes of 2–3%. Upland and bottomland areas are nearly level. The steepest slopes reach 55%, but comprise only small areas on the valley margins. The primary study catchment (R) drains 45 hectares of forested area and features a 300 m long, flat, unchanneled valley of a forested wetland above the channel head. The adjacent B and C catchments, where additional soil and groundwater measurements were made, are larger (169 and 117 hectares, respectively) and also feature long, flat, forested wetland valleys as well as Carolina Bay wetlands typical of the Upper Atlantic Coastal Plain (Fig. 1). There is field evidence of previous terracing, gully erosion, and downslope soil movement that occurred during the farming period prior to the establishment of the current timber stand.

The hillslopes and ridges are covered by longleaf pine (*Pinus palustris*), loblolly pine (*Pinus taeda*), and slash pine (*Pinus elliottii*) first established in the late 1950s, now in the second or third rotation. Mixed hardwoods dominate the riparian areas, mainly sweet gum (*Liquidambar styraciflua*). The soils are well-drained, loamy, siliceous, thermic Grossarenic Paleudults (Rasmussen and Mote, 2007), featuring a thin loamy sand A horizon overlying a deep loamy sand E horizon that grades into an argillic Bt horizon of sandy clay loam. Herein the A and E horizons will be referred to as mineral soils. The surface soils contain 80–90% sand, and clay content increases to 35% or more in the Bt horizon (Kilgo and Blake, 2005).

3. Methods

The hydrological measurements are focused in the R catchment where a 121 m interflow interception trench was excavated along the contour at mid-slope in 2009. Slopes above the trench range from about 6% to 12%. The open trench (covered by a tarp structure to prevent precipitation input) is 1.5–2.0 m deep and consists of eleven separate 11 m long trench drains constructed within the clay layer. Within each segment, a perforated pipe was covered with gravel and landscape cloth to intercept lateral flow moving above and within the argillic layer from an upslope contributing area of 5.7 ha (13% of the R catchment). Intercepted water from each drain was piped downhill into a v-notch weir box in which water level was measured by an Odyssey capacitance probe at

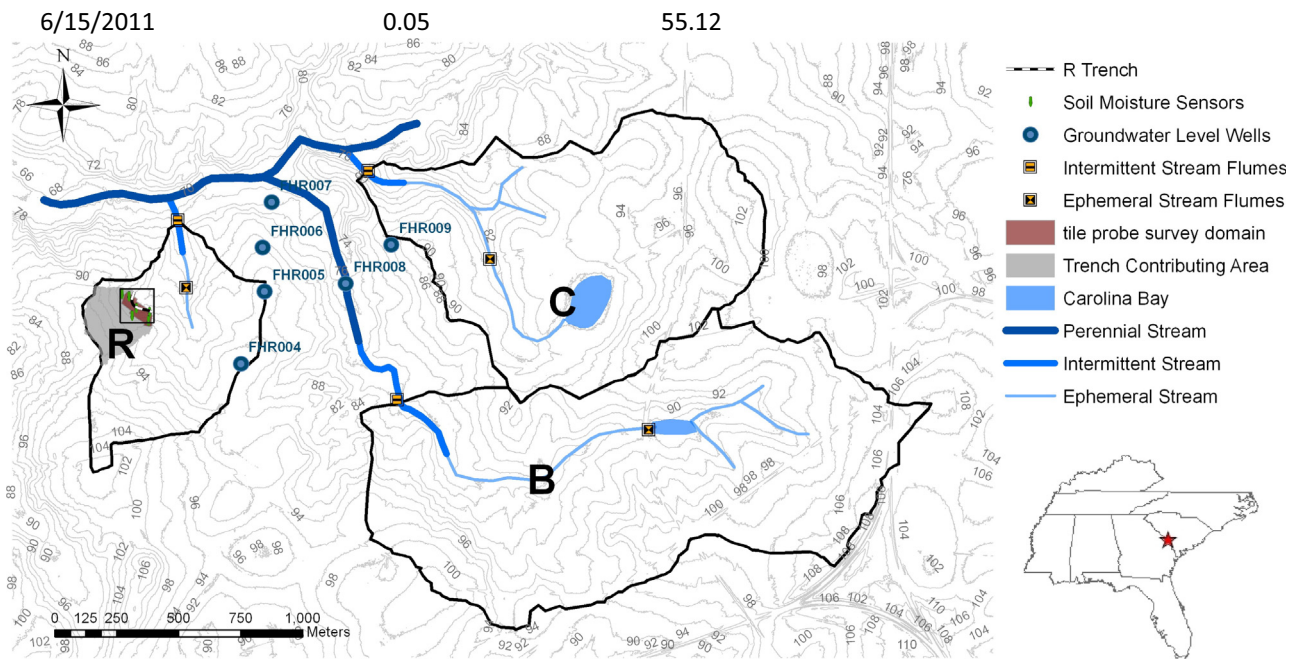


Fig. 1. Map of three study catchments (R, B, and C) in Upper Coastal Plain of South Carolina showing the locations of stream segments, the interflow interception trench in R, groundwater monitoring wells, stream flumes, piezometers nests, the argillic horizon survey domain assessed by tile probe, and soil moisture sensors. Catchment R is where the majority of the research was conducted. The black square box indicates the area where depth-to-argillic layer surveys were conducted and max-rise piezometers were located. Readers should refer Fig. 7 for details in the area. The 1 m contour line is surface elevation.

10-min intervals (Dataflow System, New Zealand). We conducted walk-through inspections of the trench and drains during or after storm events. The walk through inspections determined whether macropore flow was exiting the trench face and where the upslope trench face was wet.

Depths to the argillic layer were characterized by two different methods: trench face inspection and tile probing. First, the argillic surface was identified by visual and tactile inspection at 0.5 m intervals at the R catchment trench face as well as in two other trenches in the B and C catchments, yielding a total survey length of 200 m (400 measurements). Depth to the argillic layer was also mapped on a 2 m by 4 m grid (838 measurements) on the hillslope above the R trench by pushing a tile probe into the soil until it reached the argillic layer. In 2011, additional tile probe testing (585 measurements) was conducted on a 2 m by 1 m grid within a 40 m by 40 m sub-domain above trench drain segments 4 through 6. Multiple people were involved in the measurements, but each did a series of calibrations with known argillic depths at the trench face to gage the resistance associated with the change in texture. When the argillic layer was encountered, much greater force was needed to advance the probe. However, the probe could also be stopped by rocks or roots, so three measurements were taken at each point, and the deepest penetration was recorded. High-quality LiDAR data (0.877 m spatial resolution and 0.015 m root mean square error) and fine scale detection of depth to the argillic layer by tile probe allowed the creation of high-resolution maps of the surface and argillic horizon. Soil profiles were characterized for texture and color in each horizon by augering down to 2 m depths throughout the hillslopes and riparian zones. In-situ hydraulic conductivities (Ksat) in the A horizon (8 measurements), mid-layer (5 measurements), and the argillic horizon (6 measurements) were measured across the catchment using compact constant head permeameter (CCHP, or Amoozometer). Soil moisture characteristic curves for topsoils and the argillic layer were developed on intact cores using the hanging water table method, and

van Genuchten parameters α , n , and m were fitted to the resulting data (van Genuchten, 1980). The van Genuchten soil hydraulic model is defined as:

$$\theta = \theta_r + \frac{(\theta_s - \theta_r)}{[1 + (\alpha h)^n]^{1/m}}$$

where θ is volumetric soil water content, θ_r is residual water content, θ_s is saturated water content, h is the matric potential (kPa), and α , n , and m ($m = 1 - 1/n$) are empirical parameters.

Three 1 m wide and 10 m long trenches were cut down into the argillic layer with a backhoe at the top of the R catchment and on two hillslopes in the lower B catchment. At these trenches, the argillic layer was visually inspected for areas of anomalous color, texture, and obvious root penetration (Fig. 2b and c). The thickness of the argillic layer was measured by augering through the argillic layer at seven locations in the hillslope above the R trench and in two other locations in the adjacent watersheds.

To examine groundwater dynamics, four nests of piezometers were installed on the hillslope above the trench in the R catchment with one piezometer above the argillic layer, one within the argillic layer, and one below the argillic layer in each nest. Each piezometer was equipped with an Odyssey capacitance probe to measure water depth at 15-min intervals. In addition to the recording piezometers, 48 maximum rise piezometers in a regular grid of 12 rows by 4 rows going upslope were installed on the same hillslope. They were checked monthly to determine maximum groundwater level in the preceding month. Maximum water level was determined by measuring the height to which water washed away cork dust that was placed on a central rod in the piezometer. The cork dust was reapplied every month. Six riparian piezometers were installed near the stream gauges to a depth of 1.8 m to monitor riparian groundwater dynamics and were measured manually on monthly basis. An H-flume was installed at the R catchment outlet and water level was recorded using an ISCO 6712 automated sampler (Teledyne ISCO, Lincoln, NE) to calculate streamflow. Six

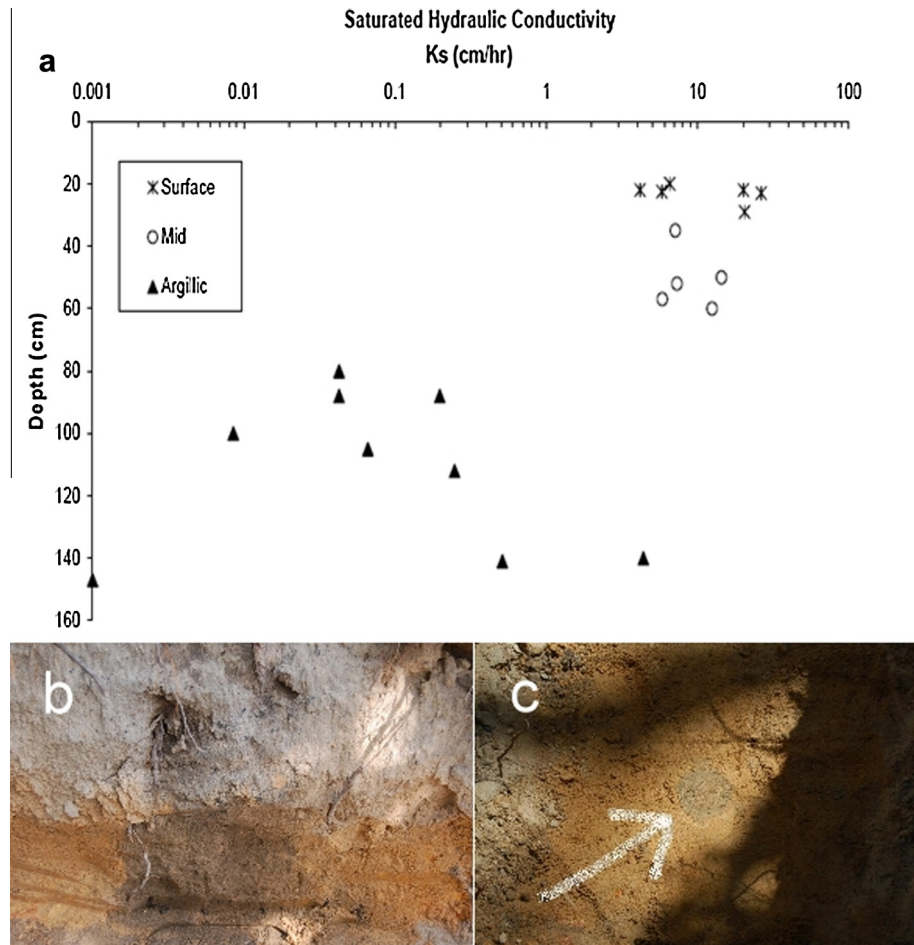


Fig. 2. a. Saturated hydraulic conductivity (K_{sat}) by depth for the surface, mid, and argillic layers. K_{sat} measurements were determined using the compact constant head permeameter (CCHP); b. vertical soil profile at trench excavation (~1 m high); c. bottom of an excavation with an anomaly (as arrow pointed, ~0.1 m in diameter).

nests of ECH₂O soil moisture probes, (Decagon Devices, Pullman, WA) were arranged to monitor soil volumetric water content (VWC) at both the soil surface and at the top of the argillic layer above the trench. Soil water storage accounting for interflow initiation was estimated by precipitation records from a meteorological tower at SRS (Central Tower 200F), approximately 1.6 km away from the catchments. The regional surficial groundwater table, flowing through unconsolidated sands and clays of the Upper Three Runs Aquifer, was measured every 4 h using Global Water WL16 and WL15 water level loggers (Global Water Instrumentation, Inc.) that were placed in two wells on the eastern ridge of the R watershed and in four wells in the lower B watershed. Well depths ranged from 4.7 to 14 m as the location of the wells varied from areas close the riparian zones to the ridges of the watersheds.

Saturated interflow travel times were calculated along flow pathlines starting from the valley margins up to the ridgelines. Valley margins were defined by the extent of the Pickeny sand and Ogeechee sandy loam soils. Both valley soil series were mapped by the Natural Resources Conservation Services (NRCS). At each increment along the pathlines, pore-velocities were calculated based on the local slope, a porosity of 0.35, and the highest and lowest bulk A and E horizon conductivities determined from observed trench outflow rates (223 cm/h and 33 cm/h, respectively; described in detail in Section 4). A contour map of the resulting travel times was created from the resulting net of travel times.

4. Results

4.1. Saturated hydraulic conductivities and soil moisture characteristic curves

The loamy sand topsoils were well drained with a median hydraulic conductivity (K_{sat}) of 10 cm/h and a range spanning over one order of magnitude. In contrast, the median K_{sat} in the argillic layer was 0.5 cm/h, and varied over four orders of magnitude from 0.008 cm/h to 5 cm/h. Six out of eight K_{sat} measurements in the argillic layer were two orders of magnitude lower than the median value for topsoil (Fig. 2a). Soil moisture characteristic curves contrasted sharply between the loamy sand topsoil and the sandy clay loam argillic layer (Fig. 3). As expected from the textures, topsoils lost most of the water at higher potentials and retained less than 3% of moisture at –100 cm pressure head. Clay soils, on the other hand, were able to hold significantly more water (>25%) throughout the tested pressure range. Van Genuchten's parameters were derived by fitting the core sample measurements in sand and clay (Table 1), which helped quantifying the differences in the hydraulic characteristics of the A/E and Bt horizons.

Examination of the vertical distribution of soil texture indicated that the transition from the sandy topsoil to the clayey subsoil was gradual and usually lacked a distinct boundary. In some cases, clay content increased gradually, and the soil profile included a BE transition horizon. The transitional characteristics of the argillic interface imply lateral flow can move within the argillic layer as well as

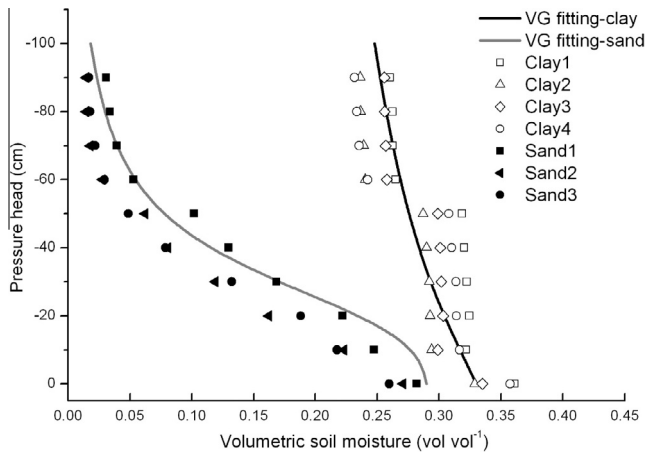


Fig. 3. Moisture release curves of the surface (sand) and argillic (clay) layers were fitted with van Genuchten curves. Data were obtained from soil columns that maintained a constant negative pressure head on each soil core.

Table 1

Van Genuchten's parameters derived by fitting the soil moisture release curve of argillic and sand layers of the catchment soils.

	<i>A</i>	<i>n</i>	<i>m</i>
Sand	-0.035	3.180	0.686
Clay	-0.033	1.207	0.171

above it. In fact, water regularly was observed to seep out of the trench faces below the argillic interface during storms. Visual observations of roots on the trench face and from wind-thrown trees in the forest indicated that some tree roots extended deep into or through the argillic layer. Trench excavations revealed that abnormal soil columns (anomalies) with distinctly different texture, color, and organic matter content occurred randomly in the argillic layer (Fig. 2b and c). The anomalies were notably darker in color and had coarser particle size distributions. Ksat tests by CCHP at six locations indicated these columns had much higher Ksat (two orders of magnitude) than the surrounding clay. Possible processes that created these anomalies are the decay of tree roots, including tap roots, and/or animal burrowing. The loamy sand topsoil lacks cohesion and tends to collapse and infill these anomalies in the underlying argillic layer.

4.2. Hillslope and subsurface topography and depths to the argillic layer

The trench hillslope had a relatively steep average gradient of 7% (compared to the flat topography of the entire catchment) and maximum slopes of around 12% with little undulation at the surface and irregular argillic topography compared to the surface (Fig. 4). Mean depth to the argillic layer within this hillslope was 0.76 m, but ranged from 0.19 m to 1.62 m. Transects of depths to the argillic layer measured at high spatial resolution (0.5 m) on the R, B, and C trench faces (Fig. 5 and Table 2) revealed an undulating argillic surface with large variation over short spatial scales. Depths to the argillic layer across both measurement approaches (depth at trench face, tile probe depth above trench at 1 m by 1 m and 2 m by 4 m scales) ranged between 0.15 m and 2.00 m, with median values of 0.50–0.80 m. Standard deviations were high relative to the mean values and ranged from 0.10 m to 0.40 m. Depths to the argillic layer were usually symmetrically and near-normally distributed, except in the R catchment (Table 2) where they displayed a long right tail. Both the trench transects and the detailed soil depth map indicated that the argillic layer surface was very irregular and dimpled.

The thickness of the argillic layer varied from 1.3 to 3.0 m, with a mean and median of 2.1 and 2.0 m, respectively. Auger borings through the argillic layer also indicated variability in the texture, structure, cohesiveness, and color. For example, most of the argillic layer was friable sandy clay loam with color ranging from 2.5YR 5/6 reddish brown to 10YR 5/6 light yellowish brown yellow-orange, but we encountered occasional layers of very hard, cemented, reddish-purple to purple (not in the Munsell soil color books) clay. Some borings revealed lenses of river-washed gravels within the sandy clay loam argillic layer.

4.3. Groundwater perching, soil moisture, and interflow behavior

Piezometers above and within the argillic layer indicated that groundwater perching always began in the argillic layer and then moved upwards into the topsoil as storm size increased (see 'in argillic piezometer water level' in Fig. 6). Perching in argillic layer started 1–2 h earlier than in top soil during the two events of June and August, 2010 (Fig. 6a and b). Perching of water occurred frequently in the argillic horizon, e.g., four times in the dry summer months of 2010. The below-argillic piezometers did not respond to storm events and no connection was observed between the perched water and the regional groundwater table during the more than four years of monitoring. Depth to the regional water table was 35 m (74 m.a.s.l.) on the ridge tops and usually more than 18 m (68 m.a.s.l.) within a pre-1950 hand-dug well, at approximately the same elevation as the trench, in a 2010 summer survey. Groundwater depths below the ridge showed gradual seasonal variation of up to 2 m.

Monthly maximum water level measurements in the piezometer grid showed high spatial and temporal variability in both magnitude and frequency of perching above the argillic layer (Fig. 7). All piezometers responded (i.e., contained water) during at least some monthly measurements and no piezometer responded continuously across all monthly observations. The piezometer response frequency, defined as percent of month that piezometers contain water, ranged from 18% to 91% across the 3-year long measurement period. In other words, perching occurred every 1.1–5.5 months in various piezometers. We observed that some piezometers contained water for extended periods between storms, but few were wet only for short amounts of time in wettest periods. Piezometer records showed some seasonality despite evenly distributed precipitation throughout the year. More piezometers responded during the winter than in other months that is likely due to lower evapotranspiration. The topography of the top of the argillic layer is more irregular than the soil surface, and piezometers in argillic depressions captured more frequent perching of infiltrated water. Because of the spatial heterogeneity of Ksat in the argillic layer, some piezometers were filled with water frequently, but did not hold water long because water likely percolated through the clay or moved downslope. Soil moisture responded nearly instantaneously to precipitation and dropped back to low values (0.03–0.08 vol vol⁻¹) within a few days following storms in both the topsoils and clays (Fig. 6).

Inspection during storms never revealed macropore flow exiting the trench face. Matrix seepage was generally observed from the BE transition layer and within the argillic layer itself. Lateral flow frequency and magnitude varied among the 11 trench flumes. During storm events, flumes 1, 4, 5, and 7 were the first to respond, while others (segment 3, 9 and 10) did not respond to small to moderate storms (>60 mm, Fig. 7). The variability of lateral flow generation along the trench face indicates that the undulation of argillic layer topography influences the subsurface flow distribution and can be identified by the argillic boundary line at the trench face (Fig. 5). The argillic interface at the excavation had multiple depressions that were more than 1.5 m deep at segments

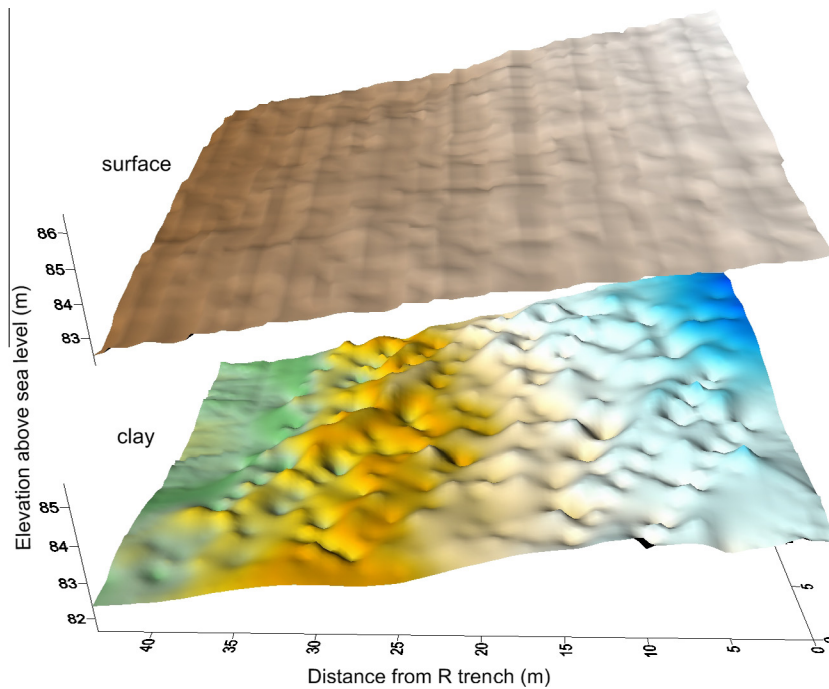


Fig. 4. Surface and argillic layer topography mapped using LiDAR and a tile-probe survey, respectively, show variation of the surface and argillic layers of an approximately 40 by 40 m area above trench segments 3 to 6 in the R catchment. A few augering tests indicated that the thickness of argillic layer ranged from 1.3 to 3.0 m. Note: the elevation of the surface layer has been lifted to better illustrate the variability in the argillic layer. Note: blue indicates high elevation and green indicates low elevation. (For interpretation of the references to color in this figure legend, the reader is referred to the web version of this article.)

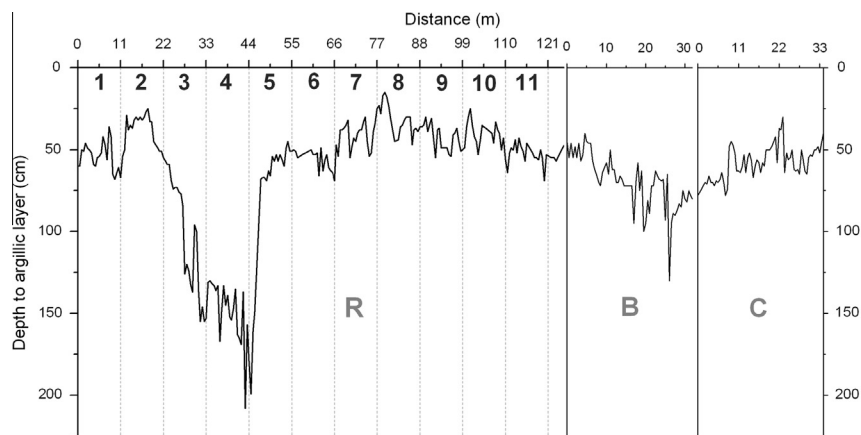


Fig. 5. Argillic boundary along the face of the R, B, and C trenches. Depths to the argillic layer ranged from 0.15 to 2.00 m, with median values in the range of 0.50–0.80 m. The larger numbers in the R trench figure show the 11 trench segments and corresponding drains. The argillic surface is irregular, and creating subsurface depression storage contributing to large fill-and-spill thresholds.

3 and 4. The perforated pipes were buried at 1.5–2 m below surface and in some cases lateral flow may move below the pipes. Accordingly, segment 3 collected flow less frequently than others. Combining the responses of trench flow with the perching water level above the trench, we observed that neither perching nor interflow follows surface topography, and perching upslope does not necessarily lead to downslope interflow (Fig. 7).

During some storms, outflow volumes from the trench exceeded streamflow volumes for the same period (Table 3), indicating a disconnection between the hillslopes and the stream. This mismatch between trench flows and streamflows occurred during both summer and winter storms. For example, the 61 mm storm on November 11th, 2009 produced greater flow volume from the trench (61.5 m^3) than from the stream (9.0 m^3) in the R catchment. The largest observed flow rate from individual 11 m trench segments ranged from 0.1 to 0.7 L/s. This is consistent with Darcian

estimates of maximum possible flow rates. If we assume 1.0 m of interflow-carrying soils (i.e., soil depth that includes the transitional zone plus part of argillic layer) and a slope of 0.10 (at the high end of slopes in the trench hillslope), then a flow rate of 0.1 L/s suggests a lateral hydraulic conductivity of 33 cm/h (at the very high end of the measured values). But a flow rate of 0.7 L/s suggests a lateral conductivity of 223 cm/h, an order of magnitude higher than our topsoil measurements. The observed flow rates indicate that our CCHP measurements of topsoil conductivity may be low-biased. The bias may be due to the error of CCHP method or the lack of representation of preferential flow. Under these same assumptions, the range of Darcy velocities would be only 3.3–23 cm/h, indicating the difficulty of driving a large amount of interflow on a 10% slope over the duration of a rain-storm. Analysis of interflow responses to storm precipitation input reveals that individual interflow pathways may be activated during

Table 2

Depth to the argillic layer (m) in interflow interception trenches and the maximum rise piezometer grid in the hillslope above the R watershed trench.

	Median	Mean	Min	Max	St. Dev.	Number of measurements
R trench	0.51	0.63	0.15	2.08	0.40	221
B trench	0.69	0.69	0.30	1.30	0.16	65
C trench	0.57	0.57	0.30	0.78	0.10	65
Detailed mapped region of R hillslope by tile probe	0.76	0.76	0.19	1.62	0.23	838
Large scale tile probegrid (2 m × 4 m)	0.76	0.77	0.56	1.50 ^a	0.32	585

^a Length of tile probe used in large scale measurements was 150 cm. The finer scale measurements used a 200 cm probe at the deeper locations.

smaller storm events, but rainfall input has to reach 60 mm in order to generate substantial interflow (Fig. 8). Estimation of downslope travel distances based on the ratio of downslope Darcy velocities to percolation velocities (Jackson et al., 2014), indicates that saturated interflow is unlikely to travel more than about 30 m on this slope due to low slopes and leakage through anomalies, similar to the leakage through fragipan cracks studied by Parlange et al. (1989). These short downslope travel distances partly explaining the mismatch between interflow behavior on this hillslope and flow observed in the stream.

5. Discussion

5.1. A perceptual model of hillslope connectivity for low-relief watersheds

The topography of the argillic layer in the 3 study catchments (R, B, C) is complex and undulating with high variation (as much

as 2 m) over short distances (<10 m). This topography results in many depressions for water storage that need to be filled before perched water can connect and spill to lower elevations. The undulating subsurface topography combined with low permeability of the confining argillic layer creates a fill-and-spill process similar to that observed above bedrock in steeper catchments (Tromp van Meerveld and McDonnell, 2006c). The fill-and-spill theory was built upon the observation that bedrock depressions will hold water until the perching level in low spots rises and spills over the local high points in the bedrock microtopography; only after saturated areas are connected will subsurface flow occur. The connectivity of saturated areas in this hillslope is very difficult to predict from gridded measures of the argillic layer topography because of the small spatial scale and randomness of the variation in the depth to the argillic. Unlike many other study areas characterized by an underlying restrictive layer (Ali et al., 2011; McDaniel et al., 2008; Redding and Devito, 2010; Tromp van Meerveld and McDonnell, 2006b), the impeding layer at SRS appears to have many areas of vertical preferred flow throughout it (Fig. 9). The high variability in both the argillic topography and conductivity sets the template for near-surface hydrologic behavior in this landscape. The origin of the variability in the argillic surface is unknown, but we hypothesize that the variability originates from a combination of root penetration and subsequent rot; lifting of portions of the argillic surface when trees fall; and also animal burrowing and subsequent infill. Given that these hillslopes have been forested throughout the Pleistocene, there has been sufficient time for tree falls to create a mosaic of overlapping divots in the argillic surface. More work is needed to understand the history of soil evolution under natural and managed conditions as suggested by Tani (2013) in order to have a comprehensive understanding of interflow behavior.

Notwithstanding our lack of detailed slope evolution history, our work suggests the following sequence for subsurface redistribution of rainfall as storm size increases: (1) rainfall infiltrates

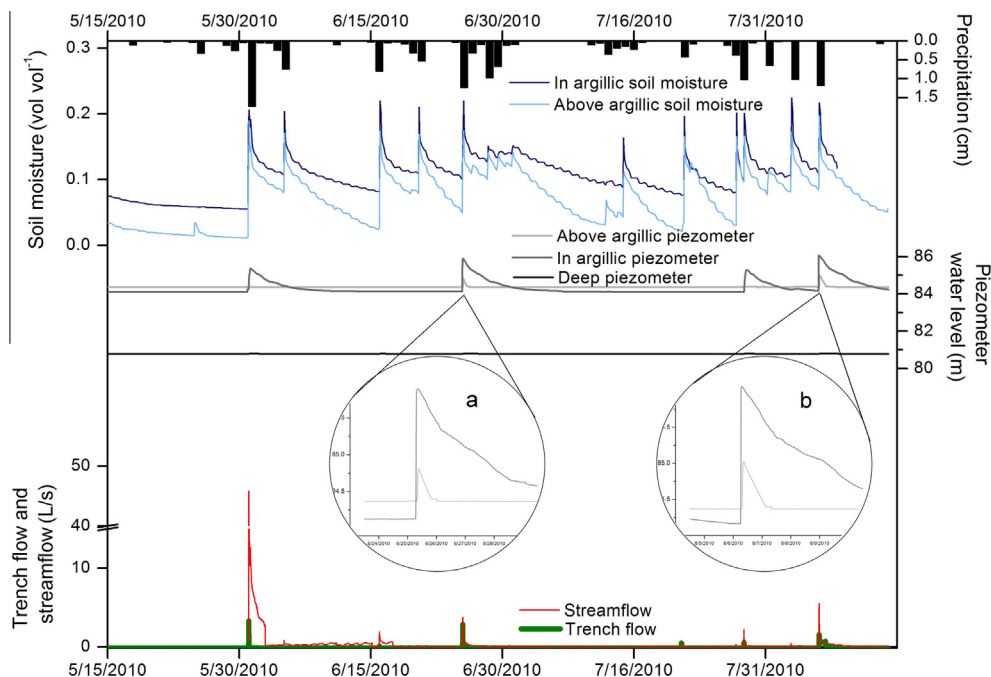


Fig. 6. Hydrological responses (from top to bottom) to precipitation in the summer of 2010 (5/15/2010 to 8/15/2010): a piezometer nest at three depths, soil moisture above and in the argillic layer, lateral flow intercepted by the R trench, and streamflow at the outlet of the R catchment. Perching was observed more frequently in the argillic layer than below the argillic layer. Subplot 6a and 6b are enlarged view of two events when both piezometers above and in the argillic layer responded. The occurrence of trench interflow and streamflow in the R catchment corresponded to perching (e.g., the response of the in-argillic piezometer and trench flow were similar). The trench contributing area only represented approximately 13% of the entire catchment, but interflow volume was comparable to streamflow except during the late May and early August events, suggesting that the contribution of upslope shallow subsurface water to stream flow is rather small.

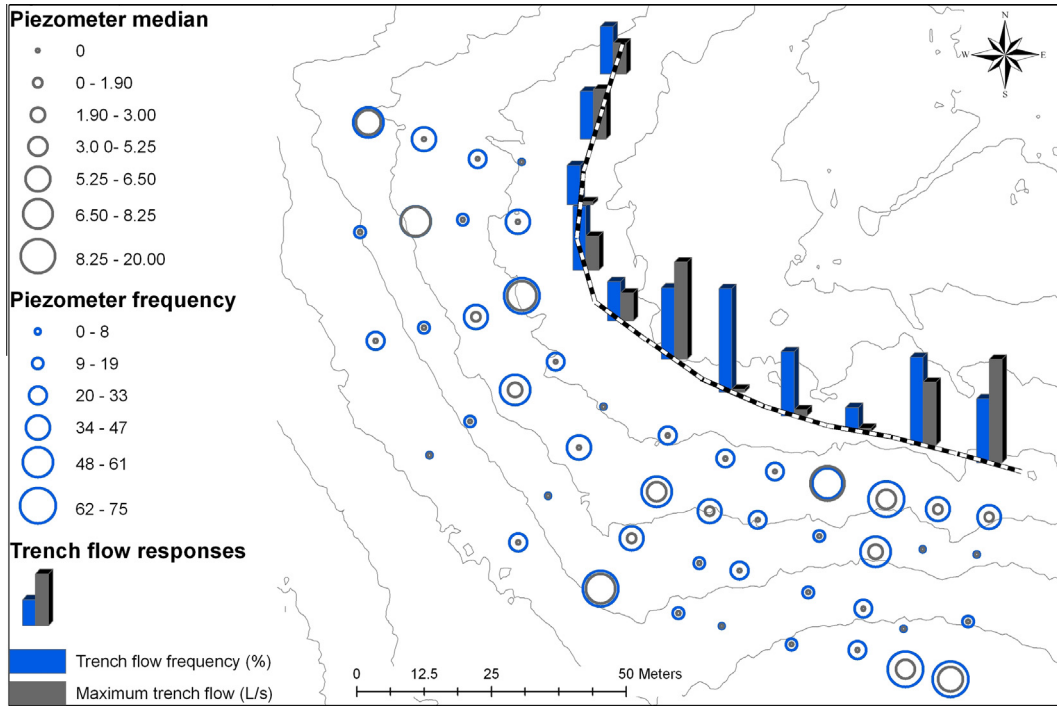


Fig. 7. The response of the maximum rise piezometers and the trenches to storms from 2009 to 2011. Gray dots indicated median level of water of all detectable events in the piezometers above R catchment trench (segmented line). Blue circles indicated frequency of water occurrence in piezometers in all months over 3-year period. Blue bars were frequency of flow occurrence of total months and ranged from 9% to 27%, gray bars represented maximum trench flows. The frequency of trench flows was counted only after flows were >0.05 L/s. Underlying was a 1-m contour lines. (For interpretation of the references to color in this figure legend, the reader is referred to the web version of this article.)

Table 3

Trench flow and streamflow responses of all trench flow events during the period of June 2009 to June 2011 (italicized numbers indicate that trench flow was greater than streamflow).

	Trench flow (m ³)	Streamflow (m ³)
6/19/2009	0.15	9.31
7/6/2009	22.26	1.31
11/11/2009	61.51	8.96
12/3/2009	2.85	1.86
12/19/2009	29.33	96.05
2/25/2009	545.27	2047.50
1/22/2010	39.70	365.36
2/7/2010	7.39	130.64
3/13/2010	14.89	2.76
5/31/2010	7.92	1048.50
6/16/2010	0.34	69.09
6/25/2010	25.18	76.16
7/21/2010	0.63	3.20
7/28/2010	1.94	14.54
8/7/2010	<i>165.61</i>	<i>104.69</i>
2/5/2011	131.16	1374.30
6/15/2011	0.05	55.12

rapidly, and the wetting front propagates vertically until it reaches the argillic layer; (2) the argillic layer saturates from within, and subsequently localized patches of perched water tables develop; (3) depressions in the argillic horizon surface are filled and connect locally as lateral flows are initiated at limited locations; (4) most depressions are filled and widespread hillslope connectivity is formed. At the third stage, we saw interflow entering a few trench sections, and as the last stage was reached, we saw interflow entering most trench sections. However, on the hillslopes, much of the storm water percolates through anomalies in the argillic layers. This sequencing is consistent with the general sequencing of runoff of all slopes as outlined recently by McDonnell (2013).

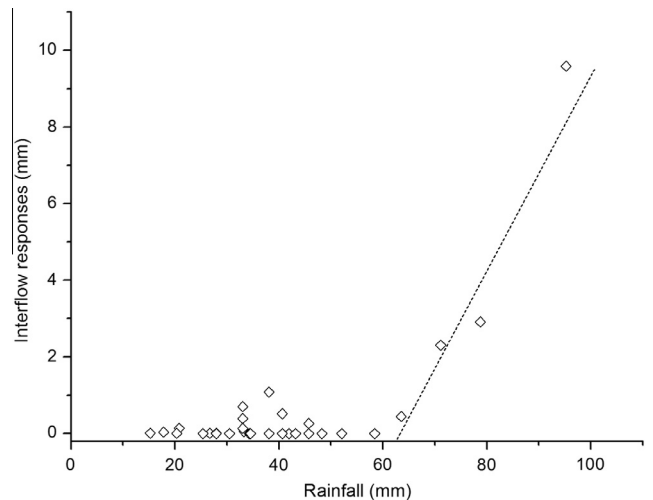


Fig. 8. The response of interflow to rainfall events. Interflow was initiated when rainfall exceeded 60 mm. Only storm events greater than 10 mm were included in this figure.

Relatively high forest evapotranspiration demand in this climate means that the soils rapidly dry out and reset the interflow thresholds between storms. The high amounts of subsurface storage in the low points of the argillic surface may act to improve tree growth and productivity in this landscape by acting as reservoirs to supply transpiration demand as measured by Tromp van Meerveld and McDonnell (2006a) at the nearby Panola hillslope.

When the topography above a trench segment is comprised of deep or multiple depressions as suggested by the argillic boundary at the trench face (Fig. 5) and the depth-to-clay survey above segment 3 and 4 (Fig. 4), some water is dammed and confined in the

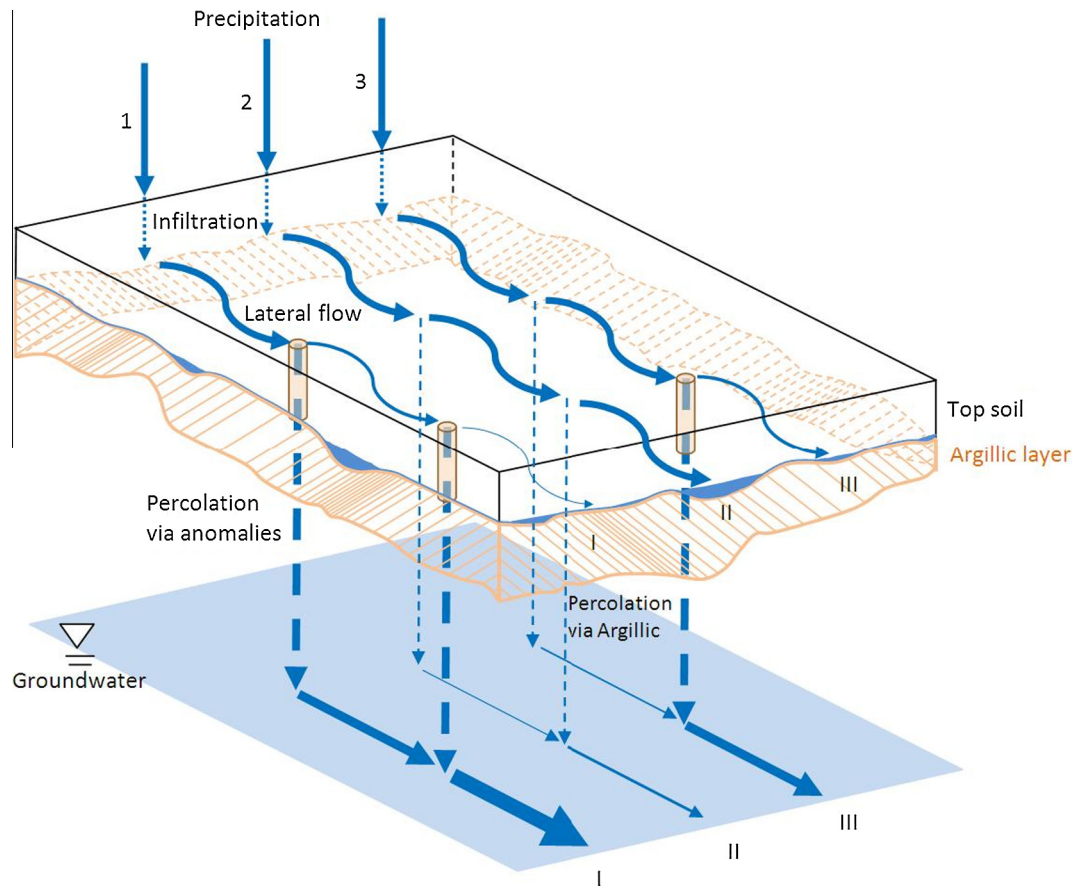


Fig. 9. Conceptual connectivity model at the hillslope scale indicates that the storm water flowpath follows a series of progressive steps as storm size increases: (1) the input necessary to bring the mineral soil profile up to field capacity near the soil base, (2) to then bring the upper part of the argillic layer to saturation, (3) then to fill the depressional storage in the argillic layer surface and, (4) then to connect the depressions across the slope. The incoming water is partitioned into interflow and deep percolation (neglecting ET and storage change) and segments I, II, and III have different volumes of outflow at the argillic interface and groundwater influenced by upslope Ksat discrepancies. Segment I has the lowest outflow because of the most percolation was lost via anomalies, while segment II has the greatest outflow due to the lack of anomalies.

depressions. The corresponding downslope segments will be less responsive than those with relatively flat contributing argillic topography. Alternatively, if there are anomalies (which have much higher permeability compared to surrounding argillic layers) on the route of lateral flow, the high percolation through the argillic layer may decrease the portion that reaches downslope areas (Fig. 9, segment I). If fewer argillic anomalies occur along the route, more lateral flow may appear (Fig. 9, segment II and III). The results suggest that predicting hillslope flowpaths requires not only information about surface topography and topsoil characteristics, but also information about subsurface topography and leakage rates. The high spatial variability of interflow and depressional storage also means that interflow contributions to valley water are an ensemble of substantially varying signals. One of the distinct characteristics of this hillslope compared to earlier interflow studies is the interspersed “holes” (anomalies) that filled with highly permeable sand. The anomalies not only increase subsurface storage, but also create large variation of interflow at the space of the hillslope.

The mismatch between interflow generation amounts and streamflow runoff response ratio (~ 0.02) suggests that while hillslopes “turn on” in certain places (like the measured trench section), the hillslopes are not connected to the streams at the space scale of the entire catchment and at the time scales of storm events. Thus the majority of rainfall on the catchment hillslopes results in a broad patchwork of transient saturation that percolates through argillic layer to recharge deep groundwater. This deep groundwater bypasses the first order streams and appears far

down valley as evidenced by a runoff ratio of 0.20 at the first downstream USGS gage on Fourmile Creek (#02197334, draining 15.6 km²) and a runoff ratio of 0.39 at the lower USGS gage on Fourmile Creek (#02197344, draining 58 km²). The high measured interflow initiation threshold for the trench and the low streamflow volume relative to trench flow strongly implies that steeper hillslope segments directly adjacent to the riparian zones likely to contribute to channel stormflow in the stream (Fig. 6), a finding supported by water isotope analysis by Klaus et al. (2015) and downslope travel distance analysis by Jackson et al. (2014). This is largely attributed to low hydraulic gradient (flat terrain) and low conductivity contrast between top soil and impeding layer (high permeability in argillic layer induced by anomalies). Over most of the hillslope, interflow acts only to transfer water downslope before it percolates to groundwater (Jackson et al., 2014). Interflow producing events on site last hours to a few days (up to a week), and only the hillslopes on the riparian margins can contribute interflow to the valleys on the time scale of an interflow event (Fig. 10). Potential interflow travel times from the majority of the watershed area exceed 50 days even at the highest conductivity estimate of 223 cm/h.

5.2. Storm size threshold for lateral flow initiation

The A/E horizon thickness averages 0.8 m, which is comparable to soil depths at other well-studied hillslopes, such as the Maimai (New Zealand) (Graham et al., 2010) and Panola catchments

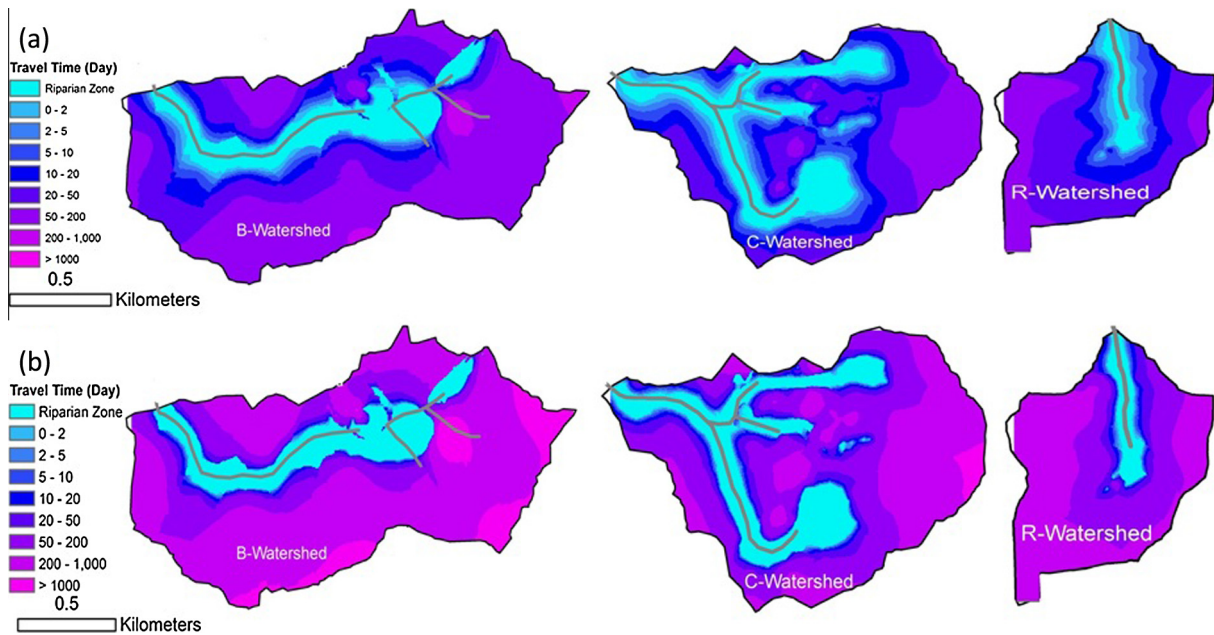


Fig. 10. Cumulative saturated interflow travel times calculated along flow paths from the riparian boundary to the ridgetops based on local slope at each point along the flowpath, a porosity of 0.35, and saturated conductivities of (a) 223 cm/h or (b) 33 cm/h (see Section 3 for more detailed description of travel time calculations). Travel times from hillslope segments on the margin of the riparian zones to the stream are within the duration of interflow events. Saturated interflow travel times from the majority of the watershed exceeded 50 days even at the higher conductivity of 223 cm/h. At the low end of the estimated conductivities, saturated interflow travel times exceeded 200 days across most of the catchments.

(Tromp van Meerveld and McDonnell, 2006b), and thinner than the mineral soil at the Watershed 10 hillslope, HJ Andrews experimental forest, Oregon (McGuire and McDonnell, 2010). The loamy sand mineral soil at SRS drains quickly and holds only a few percent of water by volume at field capacity. Excavation of tree roots and diurnal variation of soil moisture in the argillic layer suggests the pines may utilize the argillic layer as a water resource. In the growing season, the upper part of the argillic layer can become very dry with soil volumetric water content (VWC) dropping from 30–40% in wet conditions to 5% in dry conditions. Our piezometer observations indicate that perching begins within the argillic layer itself, and when the argillic layer is very dry, more water is needed to wet up the argillic layer before perching occurs. Because of the wetting needs and greater water holding capacity of the argillic layer compared to the mineral soil, the threshold for initiating perching in the argillic layer is dependent on the moisture condition of both the argillic layer and the mineral soil above.

The rainfall threshold for interflow generation at the trenched slope derived from field measurements is approximately 60 mm (Fig. 8). This value is nearly identical to the value noted by Tromp van Meerveld and McDonnell (2006a) for Panola and higher than values for steeper slopes in New Zealand (Graham et al., 2010; Mosley, 1979; Woods and Rowe, 1996) and Japan (Tani, 1997, 2013; Uchida and Asano, 2010). The high value at SRS is likely due to the low angle terrain and leakage through anomalies in the argillic layers. Impeding layer permeability is a first order controlling factor for generating a perched water table and connectivity at the hillslope (Hopp and McDonnell, 2009). CCHP test results suggest that the median vertical Ksat of the argillic layer at SRS is approximately 0.5 cm/h, slightly higher than the bedrock Ksat of 0.1–0.3 cm/h in Maimai (Graham et al., 2010) and other study areas. The relatively high permeability of the argillic layer partially accounts for the greater threshold value because more water input is needed to compensate for percolation through the argillic layer.

6. Conclusions

The highly variable topography and conductivities of the sandy clay loam argillic layer create a hillslope system in which shallow groundwater perches frequently within and above the argillic layer, but lateral flow occurs much less frequently and does not appear to contribute substantially to streamflow during most storms. Depths to the argillic layer were highly variable over short distances, indicating large areas of subsurface detention storage. Lateral flow occurred largely as matrix flow (lateral macropore flow was not observed) moving through the BE transition layers and was highly spatially variable, with very different frequencies and volumes of lateral flow among the eleven trench sections. Streamflow pulses showed little relationship to lateral flow pulses during most storm events except a few major events (Table 3), indicating a hillslope–stream disconnect except during large events with high antecedent moisture conditions. Essentially, there are four steps in the process of interflow generation: (1) infiltrated water brings the A and E horizons to field capacity, (2) the active portion of the argillic layer saturates and perching begins, (3) depressional storage in the argillic layer surface is filled, and (4) the depressions connect across the slope as infiltration continues. What is unique here compared to original fill-and-spill theory is step 2 when the argillic layer has to be wetted up in order to start perching, while bedrock should require no such wetting process. Also filling and connecting processes in last two steps have to compete with vertical loss through argillic anomalies that are highly permeable, reducing the likelihood of exceeding the spill threshold. There are spectra of each threshold across the hillslope, and these spectra contribute to the large lateral flow response variability along the trench segments. Spatial variation in the argillic microtopography and permeability also contribute to the variation in interflow generation across the slope.

Hydrologic behavior on these hillslopes reflected a variation of the fill-and-spill process model. Tromp van Meerveld and

McDonnell (2006c) exhibiting a fill-dominated regime as suggested by Hopp and McDonnell (2009). The high frequency of concavities in the undulating argillic surface, combined with the occurrence of high conductivity anomalies within the argillic layer, created a high threshold for connecting low spots in the argillic layer and transmitting interflow downslope. Combined with the low slopes, these slope characteristics also result in short downslope travel distances for interflow, such that most of the hillslopes are disconnected from stormflow generation in streams. Only the steeper slopes adjacent to the stream valleys are likely to contribute interflow to streams on the timescale of a storm. This geological setting is common in lowland and coastal plain catchments and may imply a longer transit time of water and solutes from most of the hillslope to streams. Therefore, nonpoint source water quality issues caused by intensive silvicultural or agricultural practices (i.e., via excess fertilization) are likely delayed in these low-relief watersheds.

Acknowledgments

Support was provided by the Department of Energy – Bioenergy Technologies Office and Savannah River Operations Office through the U.S. Forest Service Savannah River under Interagency Agreement DE-A109-00SR22188. SRS is a National Environmental Research Park. John Blake of the USDA Forest Service was instrumental in project coordination. Benjamin Morris managed the field data collection. Bob Bahn, Shelly Robertson, Erin Harris, Damion Drover, Louise Jacques and several undergraduates from the University of Georgia assisted with fieldwork. Kellie Vache of Oregon State University and Luisa Hopp of the University of Bayreuth provided valuable advice and discussions of the data. Support to Natalie Griffiths was provided by U.S. DOE Bioenergy Technologies Office. Oak Ridge National Laboratory is managed by UT-Battelle, LLC for the U.S. Department of Energy under contract DE-AC05-00OR22725.

References

- Ali, G.A., L'Heureux, C., Roy, A.G., Turmel, M., Courchesne, F., 2011. Linking spatial patterns of perched groundwater storage and stormflow generation processes in a headwater forested catchment. *Hydrol. Process.* 25, 3843–3857.
- Anderson, M.G., Burt, T.P., 1978. The role of topography in controlling throughflow generation. *Earth Surf. Process.* 3, 331–344.
- Atkinson, T.C., 1978. Techniques for measuring subsurface flow on hillslopes. In: Kirkby, M.J. (Ed.), *Hillslope Hydrology (Landscape Systems: A Series in Geomorphology)*. John Wiley and Sons, pp. 70–120.
- Bachmair, S., Weiler, M., 2011. New dimensions of hillslope hydrology. In: Levia, D. F., Carlyle-Moses, D., Tanaka, T. (Eds.), *Forest Hydrology and Biogeochemistry*. Springer, Netherlands, Amsterdam, pp. 455–481.
- Beasley, R.S., 1976. Contribution of subsurface flow from the upper slopes of forested watersheds to channel flow. *Soil Sci. Soc. Am. J.* 40, 955–957.
- Buttle, J.M., McDonald, D.J., 2002. Coupled vertical and lateral preferential flow on a forested slope. *Water Resour. Res.* 38 (5).
- Devito, K. et al., 2005. A framework for broad-scale classification of hydrologic response units on the Boreal Plain: is topography the last thing to consider? *Hydrol. Process.* 19, 1705–1714.
- Engler, A., 1919. *Untersuchungen über den einfluss des Waldes auf den Stand der Gewässer*. Kommissionsverlag von Beer & Cie, Zurich, 12.
- Gabet, E.J., Mudd, S.M., 2010. Bedrock erosion by root fracture and tree throw: a coupled biogeomorphic model to explore the humped soil production function and the persistence of hillslope soils. *J. Geophys. Res.* 115.
- Graham, C.B., Woods, R.A., McDonnell, J.J., 2010. Hillslope threshold response to rainfall: (1) a field based forensic approach. *J. Hydrol.* 393, 65–76.
- Hewlett, J.D., 1961. Soil Moisture as a Source of Baseflow from Steep Mountain Watersheds. Southeastern Forest Experiment Station, USDA Forest Service, Asheville, NC.
- Hewlett, J.D., Hibbert, A.R., 1967. Factors affecting the response of small watersheds to precipitation in humid areas. In: Sopper, W.E., Lull, H.W. (Eds.), *International Symposium on Forest Hydrology*, Pergamon, Oxford, pp. 275–290.
- Hopp, L., McDonnell, J.J., 2009. Connectivity at the hillslope scale: identifying interactions between storm size, bedrock permeability, slope angle and soil depth. *J. Hydrol.* 376, 378–391.
- Jackson, C.R., Bitew, M., Du, E., 2014. When interflow also percolates: downslope travel distances and hillslope process zones. *Hydrol. Process.* 28 (7), 3195–3200.
- Jencso, K.G. et al., 2009. Hydrologic connectivity between landscapes and streams: transferring reach- and plot-scale understanding to the catchment scale. *Water Resour. Res.* 45.
- Kilgo, J.C., Blake, J.I. (Eds.), 2005. *Ecology and Management of a Forested Landscape*. Island Press, Washington.
- Klaus, J., McDonnell, J.J., Jackson, C.R., Du, E., Griffiths, N.A., 2015. Where does streamwater come from in low relief forested watershed? A dual isotope approach. *Hydrol. Earth Syst. Sci.* 19, 125–135.
- McDaniel, P.A. et al., 2008. Linking fragipans, perched water tables, and catchment-scale hydrological processes. *Catena* 73, 166–173.
- McDonnell, J.J., 2013. Are all runoff processes the same? *Hydrol. Process.* 27 (26), 4103–4111.
- McDonnell, J.J. et al., 1996. A new method for studying flow on steep humid hillslopes. *EOS* 77 (47), 465–472.
- McGuire, K.J., McDonnell, J.J., 2010. Hydrological connectivity of hillslopes and streams: characteristic time scales and nonlinearities. *Water Resour. Res.* 46, W10543.
- Mosley, M.P., 1979. *Streamflow generation in a forested watershed, New Zealand*. *Water Resour. Res.* 15, 795–806.
- Near, D.G., Ice, G.G., Jackson, C.R., 2009. Linkages between forest soils and water quality and quantity. *For. Ecol. Manage.* 258, 2269–2281.
- Newman, B.D., Campbell, A.R., Wilcox, B.P., 1998. Lateral subsurface flow pathways in a semiarid ponderosa pine hillslope. *Water Resour. Res.* 34 (12).
- Parlange, M.B., Steenhuis, T.S., Timlin, D.J., Stagnitti, F., Bryant, R.B., 1989. Subsurface flow above a fragipan horizon. *Soil Sci. Soc. Am. J.* 53 (1), 77–86.
- Pearce, A.J., Stewart, M.K., Sklash, M.G., 1986. Storm runoff generation in humid headwater catchments 1. Where does the water come from? *Water Resour. Res.* 22 (8), 1263–1277.
- Rasmussen, T.C., Mote, T.L., 2007. Monitoring surface and subsurface water storage using confined aquifer water levels at the Savannah River Site, USA. *Vadose Zone J.* 6, 327–335.
- Rebel, K.T., 2005. *Using Trees to Remediate Tritium Contaminated Groundwater: A Modeling an Tracer Study*. Cornell University, 173 pp.
- Redding, T., Devito, K., 2010. Mechanisms and pathways of lateral flow on aspen-forested, Luvisolic soils, Western Boreal Plains, Alberta, Canada. *Hydrol. Process.* 24, 2995–3010.
- Spence, C., Woo, M.K., 2003. Hydrology of subarctic Canadian Shield: soil filled valleys. *J. Hydrol.* 279, 151–166.
- Tani, M., 1997. Runoff generation processes estimated from hydrological observations on a steep forested hillslope with a thin soil layer. *J. Hydrol.* 200, 84–109.
- Tani, M., 2013. A paradigm shift in stormflow predictions for active tectonic regions with large-magnitude storms: generalisation of catchment observations by hydraulic sensitivity analysis and insight into soil-layer evolution. *Hydrol. Earth Syst. Sci.* 17, 4453–4470.
- Tromp van Meerveld, H.J., McDonnell, J.J., 2006a. On the interactions between the spatial patterns of topography, soil moisture, transpiration and species distribution at the hillslope scale. *Adv. Water Resour.* 29, 293–310.
- Tromp van Meerveld, H.J., McDonnell, J.J., 2006b. Threshold relations in subsurface stormflow: 1. A 147-storm analysis of the Panola hillslope. *Water Resour. Res.* 42, W02410.
- Tromp van Meerveld, H.J., McDonnell, J.J., 2006c. Threshold relations in subsurface stormflow: 2. The fill and spill hypothesis. *Water Resour. Res.* 42, W02411.
- Uchida, T., Asano, Y., 2010. Spatial variability in the flowpath of hillslope runoff and streamflow in a meso-scale catchment. *Hydrol. Process.* 24, 2277–2286.
- Ulanova, N.G., 2000. The effects of windthrow on forests at different spatial scales: a review. *For. Ecol. Manage.* 135, 155–167.
- van Genuchten, M.T., 1980. A closed-form equation for predicting the hydraulic conductivity of unsaturated soils. *Soil Sci. Soc. Am. J.* 44, 892–898.
- Weiler, M., McDonnell, J.J., Meerveld, I., Uchida, T., 2005. Subsurface stormflow. In: Anderson, M.G. (Ed.), *Encyclopedia of Hydrological Sciences*. John Wiley & Sons, Chichester, UK, pp. 1719–1732.
- Wilson, G.V., Jardine, P.M., Luxmoore, R.J., Jones, J.R., 1990. Hydrology of a forested hillslope during storm events. *Geoderma* 46 (1–3), 119–138.
- Woods, R., Rowe, L., 1996. The changing spatial variability of subsurface flow across a hillslope. *J. Hydrol.* 35 (1), 49–84.
- Zaslavsky, D., Sinai, G., 1981. Surface hydrology IV-flow in sloping, layered soil. *J. Hydraulics Div., ASCE* 107 (1), 53–64.